IIT-CAPP-16-06

Probing the two Higgs doublet wedge region with charged Higgs boson decays to boosted jets

Keith Pedersen* and Zack Sullivan†

Department of Physics, Illinois Institute of Technology, Chicago, Illinois 60616-3793, USA

(Dated: December 11, 2016)

arXiv:1612.03978v2 [hep-ph] 13 Feb 2017

Abstract

Two Higgs doublet extensions of the standard model, such as supersymmetry, predict the existence of charged Higgs bosons. We explore the reach for TeV-scale charged Higgs bosons through their associated production with top quarks, and their decay to boosted top jets and μ_x-tagged boosted bottom jets, at a 14 TeV CERN Large Hadron Collider and at a 100 TeV Future Circular Collider. In particular, we show the moderate $\tan\beta$ "wedge" region of parameter space cannot be probed at the Large Hadron Collider for TeV-scale $H^\pm$ because the cross section is too small. However, a 100 TeV future proton collider can close the wedge region below 2 TeV, and search for $H^\pm$ up to 6 TeV.

PACS numbers: 14.80.Fd,14.80.Da,13.20.He

* kpeders1@hawk.IIT.edu

† Zack.Sullivan@IIT.edu

I. INTRODUCTION

With the discovery of a 125 GeV boson at the CERN Large Hadron Collider (LHC) [1], one which behaves uncannily like the massive scalar of the standard model's (SM) singular SU(2) doublet, the question turns to whether an additional scale of physics can be found in a collider environment. A generic way to accommodate another scale of symmetry breaking is to add an additional scalar field, creating a two Higgs doublet model (2HDM) [2]. 2HDMs are commonly associated with supersymmetry (SUSY) [3–7], but they also show up in axion models masking strong CP violation [8, 9] and baryogenesis [10–12]. 2HDM are primarily characterized by $\tan\beta$ (the ratio of the two vacuum expectation values) and $\beta - \alpha$ (the doublet mixing angle). Symmetry breaking produces four scalar Higgs bosons (h, H, $H^{\pm}$) and a pseudo-scalar boson (A). If the fine tuning of the various parameters is minimal, then h is the lightest physical particle [13]. Given that a wide range of measurements have effectively ruled out flavor changing neutral currents at tree-level, realistic 2HDM are restricted to four general models [13], of which two are worth noting here: type-I, where all quarks couple to only one of the doublets, and type-II, where u_R^i and d_R^i couple to opposite doublets (a requirement of SUSY). We restrict our attention to type-II Higgs theories.

The SM-like nature of the recently discovered scalar boson (especially in its per-channel signal strength [14]), constrains many type-II 2HDM rather tightly to the alignment limit [15, 16]. Here, $\cos(\beta-\alpha) \to 0$, forcing $h \to H^0_{\rm SM}$.[1] If there is also a near-degeneracy in the masses of H, A and $H^{\pm}$, a natural consequence of SUSY in the decoupling limit [17, 18], then the bosons are kinematically forbidden from decaying to each other. This mass degeneracy also occurs in more generic 2HDM models which favor natural SM alignment without decoupling (e.g. softly broken SO(5) [19]). As such, we explore the degenerate mass sector, where the coupling of the heavy charged Higgs boson to the standard model is dominated by the heavy third generation.

Detecting $pp \to H/A$ is difficult as both the signal and background have identical initial and final states ($gg \to q\bar{q}$), and the resulting interference gives H/A resonances an unusual shape [20, 21] that is easy to mimic with pure QCD. Measuring H/A in association with an additional heavy quark pair eliminates this interference. For a charged Higgs boson, associated production is the leading order production mode ($pp \to H^{\pm}t(b)$), where the

[1] For $\tan\beta > 10$, non-aligned 2HDM are still allowed on a thin trajectory.

associated b can be resummed into the beam fragments. This study focuses on the cleaner $tH^{\pm}+X$ production channel, as a limit on $H^{\pm}$ is effectively a limit on all four 2HDM scalars.

Assuming quasi-degeneracy of the heavy Higgs masses, one finds [13]

$$\mathcal{L}_{\text{eff}} = -H^{+}\bar{t}(y_t P_L + y_b P_R)b + \text{h.c.}\,, \tag{1}$$

where $y_t = \sqrt{2}\, m_t \cot\beta/v$ and $y_b = \sqrt{2}\, m_b \tan\beta/v$ use running quark masses, and $P_{L/R}$ are the chiral projection operators. Appealing to naturalness, while simultaneously keeping $y_{tb} = \sqrt{y_t^2 + y_b^2}$ perturbative ($y_{tb} \lesssim 1$), leads to the expectation that

$$\tan\beta \geq \frac{\sqrt{2}m_t}{v} \qquad \text{and} \qquad \tan\beta \leq \frac{v}{\sqrt{2}m_b}\,, \tag{2}$$

which corresponds to $\tan\beta \in [0.83, 73.]$ at $Q_{\text{2HDM}} = 2$ TeV. At the center of this region ($\tan\beta = \sqrt{m_t/m_b}$) lies a "wedge" of low production cross section, where the coupling transitions from top-dominated at low $\tan\beta$ to a bottom-dominated at large $\tan\beta$. The wedge obfuscates the investigation of a large swath of interesting parameter space, as is quite evident in recent experimental searches for $H^{\pm}$ using 8 TeV LHC data [22, 23].

The situation should improve in LHC run 2, but the predictions range from slightly pessimistic for $m_{H^{\pm}} = 0.5$–$1\,\text{TeV}$ [16] to quite optimistic for $m_{H^{\pm}} = 0.5$–$2\,\text{TeV}$ [24, 25]. It is our assessment that the variations in previous estimates are primarily due to choices made when simulating a standard "track-vertex" b tag to suppress QCD background. This becomes more difficult as the mass of the charged Higgs moves above a TeV, as the bottom quark become significantly boosted, making theoretical predictions sensitive to careful modeling of real-world tagging efficiencies.

In this work, we predict the experimental reach for $m_{H^{\pm}} > 1\,\text{TeV}$ through its associated production with a top quark, and its decay to boosted top and boosted bottom jets, in both a generic two Higgs double model and in SUSY. In Sec. II we describe our selection cuts and tagging efficiencies in the boosted regime. In Sec. III we present our numerical results for the LHC at 14 TeV. We find that the LHC has limited reach to observe a charged Higgs boson, and so extend our examination to show the reach of a 100 TeV future circular collider (FCC).

II. METHODS

Given the disparity between previous predictions for the reconstruction of $tH^{\pm} \to ttb$ at large charged Higgs boson mass, this study concentrates on careful modeling of boosted bottom jets at the LHC and at a FCC. In this section, we address improvements to our existing μ_x boosted-bottom-jet tag, and detail improvements to signal selection over previous studies.

A. Bottom-jet tagging

Track-vertex tags use multivariate information from charged particle tracks to detect a b/c hadron decay vertex displaced from the interaction point. For jet $p_T = \mathcal{O}(100\text{ GeV})$, such tags have high b-jet efficiency ($\sim$70%) and excellent light jet fake rates ($\sim$0.1%) [26, 27], making them the primary method for b jet tagging at the LHC.

This performance deteriorates as jets approach the TeV regime. A highly boosted b jet has tracks which are relatively straight and very collimated, degrading their individual reconstruction efficiency. Additionally, the average number of tracks from the bottom hadron itself is fixed by branching ratios; it does not depend on jet p_T. Thus, as tracking performance degrades for TeV jets, it becomes easier to miss the limited number of b hadron tracks. Conversely, the average number of tracks inside a jet increases with p_T, since more fragmentation produces more particles. So as light jets (g, u, d, s) become harder, it is easier to find some combination of tracks which *fake* a displaced vertex [27]. This exacerbates the falling signal efficiency with a rising fake rate, driving S/B even lower. Hence, a common scheme in phenomenological studies — treating the nominal b-tag efficiency and fake rate as constant across all p_T — can lead to over-optimistic predictions for TeV-scale physics.

These realities spurred the development of the μ_x boosted-bottom-jet tag [28]. The μ_x tag is essentially an angular cut between a muon (from semi-leptonic b hadron decay) and the highly collimated jet "core" (the boosted remnants of the c hadron, along with collinear fragmentation from the b quark). The μ_x tag has been implemented in a public code for use with fast detector simulators [29]. While the maximum b-tagging efficiency of μ_x is limited by the overall branching ratio of semi-muonic b-hadron decay ($\sim$19%), its main virtue is that its signal efficiency ($\epsilon_b \approx 15\%$) and fake rate ($\epsilon_{\text{light}} \approx 0.6\%$) are flat as a function of jet

p_T once boosted kinematics turn on (p_T above 500 GeV).

Previously, we implemented the μ_x tag by utilizing the resolution of the electromagnetic calorimeter and avoided using tracks [28]. In the present study, we improve upon our prior implementation by allowing μ_x to access high-resolution angular information in tracks to locate the jet core, then calculate the muon opening angle. While we find that combining tracking with normal-resolution calorimetry does not change the tagging efficiency at 14 TeV, tracking becomes absolutely essential at 100 TeV. The large radius (6 m) and strong magnetic field (6 T) of the hypothetical FCC tracking system [30] smears the charged constituents in ϕ, reducing the correlation between charged tracks and multi-TeV tower jets.

B. Signal selection

There are two major production modes for tH^+ at a proton collider: the "4b" final state $gg \to [H^+ \to \bar{t}b]t\bar{b}$ (with $t \to bW^+$), and the "3b" final state $gb \to (H^+ \to \bar{t}b)t$. Since the 3$b$ final state is the dominant mode, accounting for at least 60% of the total cross section for all masses, the inclusive (3b + 4b) final state is a natural starting point. This requires tagging a boosted bottom jet and two tops: a boosted top jet from the $H^\pm$ decay, and a much softer, resolvable, associated top.

Using the μ_x tag to identify the boosted-b jet unavoidably selects events containing hard neutrinos from semi-leptonic B hadron decay. This smears the missing energy of any leptonically decaying tops, reducing the effectiveness of $\not{E}_T$ for top identification or reconstruction, and limiting $H^\pm$ mass resolution if the boosted top decays leptonically. These limitations are easily side-stepped by using only the fully hadronic decay of the boosted top, tagging the unique shape of $t \to W^+b$ merged into a single "fat" jet [31]. Conversely, the associated top is slow enough to be resolved into isolated daughters, so its fully hadronic final state is quite susceptible to QCD background. It is safer to resolve the associated top into an isolated lepton (e/μ) and a b jet (which is soft enough that high-efficiency track tags remain robust).

The $t\bar{t}$ portion of the inclusive final state provides multiple handles to suppress pure multijet background, leaving $ttj + X$ the dominant background (where $j = guds$). Here, the light flavored jet is both hard and "mis-tagged" as a primary boosted-b jet. This usually occurs when the jet showers $g \to b\bar{b}$, creating a real B-hadron inside a jet of light-flavor

origin. The sub-dominant background is $tt(bb/cc)$ — effectively the same final state, but with the gluon splitting at a much higher scale. Other final states (e.g. $tjj + X$ and $ttbj$) are found to be negligible.

Event reconstruction begins with jet reconstruction. First, "narrow" jets are clustered using an anti-kt algorithm with $R = 0.4$ [32], and "fat" jets are clustered using a Cambridge-Aachen algorithm with $R = 0.8$ [33]. Both boosted jets must have $p_{Tj} \geq 350$ GeV, and all jets must have $p_{Tj} \geq 20(40)$ GeV for 14(100) TeV collisions. Additionally, all jets must have $\left|\eta_j\right| < 2.1(3.0)$, so that the edge of the tracker lies outside the clustering radius of narrow jets. We require exactly one isolated lepton with $p_T^{\text{lepton}} > 15(25)$ GeV. The lepton is considered isolated if $p_T^{\text{lepton}} / \sum_i p_T^i < 5\%$ for all tracks and towers within a cone of $\Delta R < 10 \text{ GeV}/p_T^{\text{lepton}}$, as prescribed in a recent experimental search [34]. Additionally, the lepton cannot fall within a $\Delta R = R_{\text{cluster}}$ cone surrounding any of the candidate jets.

Narrow jets are sorted by p_T (high to low), and the first narrow jet which is μ_x tagged becomes the boosted b candidate. To exclude the situation where the boosted top decays leptonically (and the associated top hadronically), we require that the boosted-b plus lepton system has a mass inconsistent with a top quark ($m_{bl} > 172$ GeV). This cut is primarily used to properly model the $ttj + X$ background, but is redundant in other systems because it effectively overlaps the requirement that the lepton reside outside of the boosted-b jet.

Next, fat jets are sorted by p_T, and the first one which has a boosted hadronic top tag is the boosted top candidate. We then require that $\Delta R_{bt} \geq 2$ and $|\Delta\eta_{bt}| \leq 2$ for the two boosted candidates. The latter cut is used to restrict t-channel background from hardening the tail of the m_{bt} distribution, although it removes about a fifth of all $H^{\pm}$ (whose isotropic decay is minimally boosted in the transverse direction, due to its large mass). We do not impose any constraints on the mass of the boosted top jet, as these are already built into the boosted top tag efficiency.

We then attempt to reconstruct the associated top by finding a b jet compatible with the isolated lepton. From the set of narrow jets whose p_T is smaller than the boosted b, we take at most two jets which are b-tagged and reside outside an $R = 1.2$ cone around the boosted top (which should contain its own b jet). We then attempt to find a b-lepton system with p_T less than the boosted top, and an invariant mass consistent with a top quark missing its neutrino (70 GeV $< m_{bl} <$ 180 GeV, where the slightly elevated ceiling permits detector smearing). If two b candidates pass these cuts, the one whose m_{bl} is above 110 GeV

is selected; if both are above 110 GeV, the one which is closer to 110 GeV is selected.

The total branching ratio of the hadronic/leptonic $t\bar{t}$ decay (14%), combined with the efficiency of the two boosted flavor tags ($\epsilon_b \approx 0.14$ and $\epsilon_t \approx 0.45$) and the event shape cuts for the inclusive final state, produce an overall $H^\pm$ acceptance of $\mathcal{O}(0.1\%)$. The QCD background acceptance is an order of magnitude lower, though a more important consideration is the ratio of $ttj + X$ to $tt(bb/cc)$. For the inclusive cuts, the ratio is consistently about 5:1, which is small enough that there is no clear benefit to independently reconstructing the $4b$ final state, as was previously done [16, 24], since the process is already signal constrained at the LHC.

III. RESULTS

We calculate all cross sections using a generic 2HDM from FeynRules [35–38] with MadGraph 5 v2.3.3 [39] and the CT14llo parton distribution functions [40]. Events are showered and hadronized using Pythia 8.210 [41, 42], and reconstructed using `FastJet` 3.1.3 [43] and the Delphes 3 [30] detector simulation. For the 14 TeV analysis, we modify the ATLAS card supplied with Delphes to simulate the μ_x boosted b tag (using the `MuXBoostedBTag` module available on GitHub [29]). Both the track-based b tag and the boosted top tag are applied using a functional form of the tagging efficiency based upon jet p_T. For the track-vertex b tag, we use the run 2 efficiency from the ATLAS card (based upon Ref. [44]), and for the top tag, we use the efficiencies depicted in Ref. [31], which closely match those given in more recent publications [45, 46]. At 100 TeV, we use the FCC card supplied with Delphes (again modified to simulated μ_x), with two major changes: (i) we use the same track-vertex b tagging efficiency formula used for 14 TeV and (ii) we use a more conservative tracking domain ($|\eta| \leq 3.5$).

At both collider energies, we use Delphes' "EFlow" objects (which subtracts track energy from the calorimeter towers they strike, after both tracks and towers have their energy smeared). We then cluster jets from tracks (minus isolated leptons) and track-subtracted towers. To estimate the neutrino $\not{E}_T$ inherent to the μ_x tag, we simply double the momentum of the tagging muon [28]. This does a reasonably effective job of reconstructing the $H^\pm$ peak, allowing us to use a mass window of $[0.9, 1.15] \times M_{H^\pm}$ at both 14 and 100 TeV to capture the majority of the signal. Without neutrino estimation, the $H^\pm$ peak has a noticeably longer

low-mass tail.

A. $tH^{\pm} \to ttb$ in a generic 2HDM

We first explore the reach for a charged Higgs boson produced in association with a top quark for a generic 2HDM. We convert the leading order y_{tb} used by MadGraph to a next-to-leading order y_{tb} by using the running quark masses at one-loop in QCD [47], which shifts the center of the $\tan\beta$ wedge upwards. In Fig. 1, we show the 95% confidence level (C.L.) limit for $H^{\pm}$ exclusion at a 14 TeV LHC with 300 or 3000 fb^{-1} of data. In order to compare directly with Refs. [16, 24], we show (a) the limit obtainable on the effective Yukawa coupling y_{tb}, and (b) the corresponding region of $\tan\beta$ probed. It turns out that the only Yukawa couplings y_{tb} or values of $\tan\beta$ that can be probed at the LHC are on the border of the non-perturbative regions of parameter space.

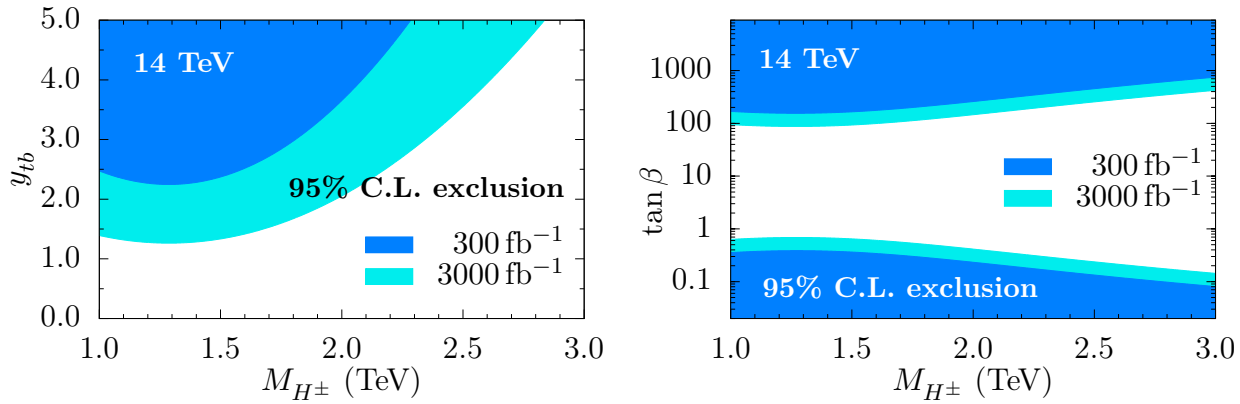

(a) (b)

FIG. 1: Predicted exclusion regime, at a 95% confidence level, for a generic 2HDM at a 14 TeV LHC in terms of (a) the effective Yukawa coupling y_{tb}, and (b) the corresponding $\tan\beta$.

The accessible region of parameter space at the LHC is entirely limited by the production cross section, as $S/B = \mathcal{O}(1/2)$ across the entire mass range. Because the $tH^{\pm}$ cross section at 14 TeV is quite small, the reach in $\tan\beta$ is poor at the LHC. Once $M_{H^{\pm}}$ surpasses 2 TeV, the $H^{\pm}$ begins to grow noticeably off-shell, which weakens the narrow width approximation we use to extrapolate from our working value of $\tan\beta$ to the 95% limit. The loss of reach

approaching 1 TeV is due to signal/background attenuation; a combination of the 350 GeV minimum p_T cut imposed on both boosted jets and the swiftly diminishing efficiency of both boosted flavor tags below 500 GeV. Given the presence of this feature, our results are consistent with extending the predictions of Ref. [16] into the TeV regime. Charged Higgs bosons are unlikely to be observed at the LHC.

The $tH^{\pm}$ cross section is strongly dependent on collider energy. A 100 TeV collider, such as a FCC, promises significantly more reach for charged Higgs bosons. At 100 TeV, the reach becomes background limited, with S/B rising from ∼1% at 1 TeV to ∼5% at 6 TeV. In Fig. 2 we observed that the reach in effective Yukawa coupling is an order-of-magnitude better than at the LHC. This allows the wedge region to close as the integrated luminosity rises above 3 ab^{-1} up to a charged Higgs mass of 2 TeV. While this analysis is robust, more sophisticated techniques — boosted decision trees (BDT) or neural nets (NN) — might improve the reach. However, since BDT/NN techniques are highly dependent on the quality of the observables with which they train, it is difficult to make accurate predictions this far from a realized 100 TeV detector system, especially using a fast detector simulator. Regardless, our results suggest that search for TeV-scale charged Higgs bosons is the domain of future colliders.

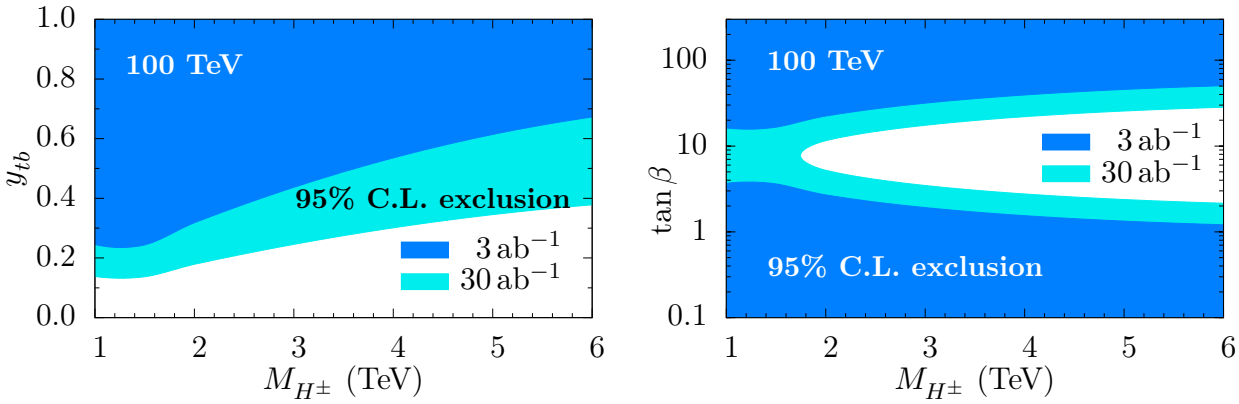

(a) (b)

FIG. 2: Predicted exclusion regime, at a 95% confidence level, for a generic 2HDM at a 100 TeV FCC in terms of (a) the effective Yukawa coupling y_{tb}, and (b) the corresponding $\tan\beta$.

B. $tH^{\pm} \to ttb$ in a supersymmetric model

One-loop corrections in the minimal supersymmetric standard model (MSSM) modify the fermionic couplings to $H^{\pm}$ bosons. The effect is most significant for the bottom quark [47, 48], and can be absorbed into the Yukawa coupling as

$$y_b^{\mathrm{SQCD}} = y_b \frac{1}{1 + \Delta m_b}\,, \tag{3}$$

(here we ignore supersymmetric electroweak corrections, using only those from supersymmetric QCD). Δm_b explicitly depends on the the gluino mass, the mass of the two bottom squark eigenstates and μ, the mass parameter coefficient of the $\epsilon_{ij} H_i^1 H_j^2$ term in the superpotential. In the quasi-degenerate limit, where all these mass parameters are of equal size, only the sign of μ survives [47]. At large $\tan\beta$ ($\sin\beta \approx 1$)

$$\Delta m_b \approx \mathrm{sign}(\mu) \frac{\alpha_s(Q_{\mathrm{SUSY}})}{3\pi} \tan\beta\,, \tag{4}$$

where Q_{SUSY} is the heavy SUSY scale (which we take to be 10 TeV, although the result is not heavily dependent upon the choice of Q_{SUSY}, since α_s runs slowly above a few TeV).

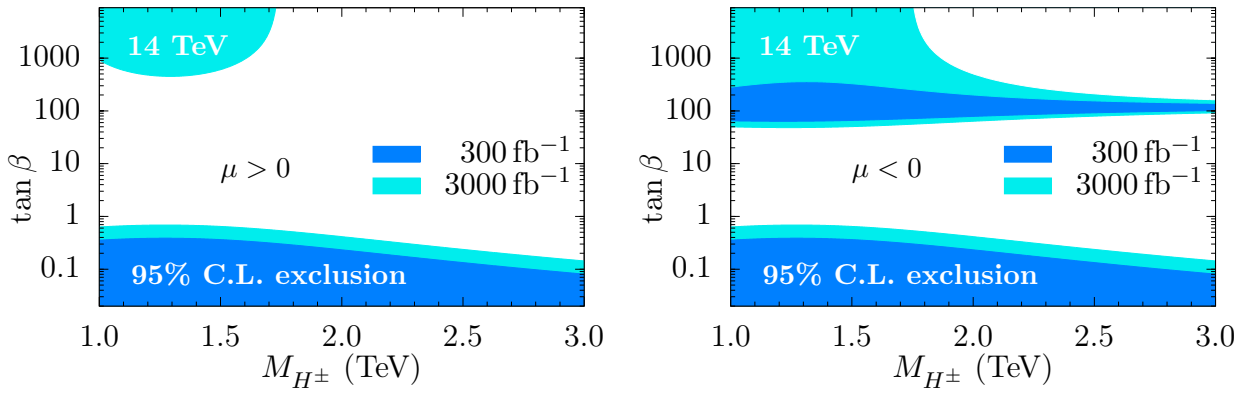

FIG. 3: Predicted exclusion regime, at a 95% confidence level, for the MSSM at a 14 TeV LHC, taking the sign of μ to be (a) positive, or (b) negative.

Comparing Fig. 3 to Fig. 1, it is readily apparent that the Δm_b correction has a significant impact on the reach at 14 TeV, where the production cross section is so small that only very large $\tan\beta$ are accessible. For a positive μ, the Δm_b correction counteracts the cross section

enhancement of large $\tan\beta$, shifting high $\tan\beta$ parameter space completely out of reach. Conversely, the negative μ correction enhances the cross section beyond the generic 2HDM in a small region of $\tan\beta \sim 100$, but decreases it at larger values of $\tan\beta$. At small values of $\tan\beta < 0.5$, the top-quark Yukawa becomes so large the theory is non-perturbative. If charged Higgs boson searches are difficult at the LHC in a generic 2HDM, in SUSY they are nearly impossible.

In stark contrast, Fig. 4 shows that the effect of Δm_b is noticeable at a 100 TeV collider, but it manifests only as a moderate shift in the upper bound of the wedge, without a dramatic change in shape. This serves to underline the nature of the Δm_b effect; for a *signal limited* search (14 TeV), it is very important, while for a *background limited* search (100 TeV) it is more-or-less negligible. The lack of sensitivity to SUSY corrections at 100 TeV demonstrates the low model dependence in the reach for charged Higgs bosons at a future collider.

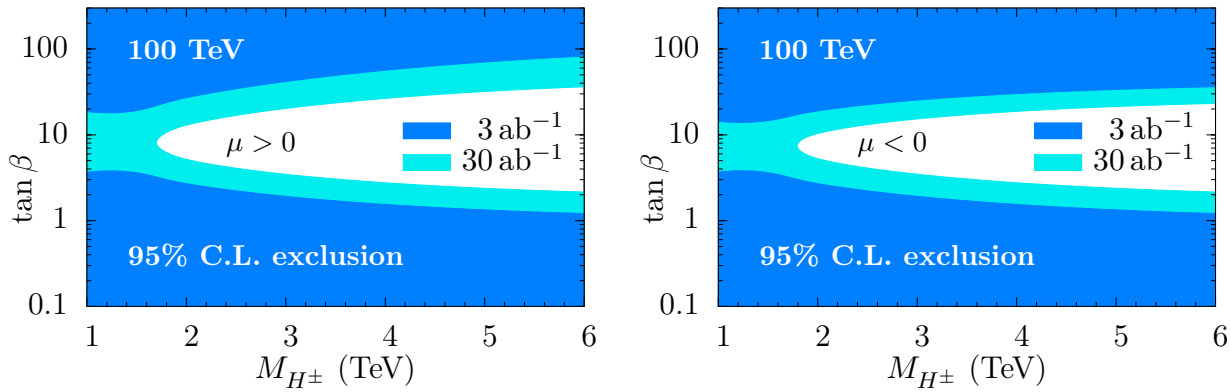

(a) (b)

FIG. 4: Predicted exclusion regime, at a 95% confidence level, for the MSSM at a 100 TeV FCC, taking the sign of μ to be (a) positive, or (b) negative.

IV. CONCLUSIONS

We examine the predicted experimental reach for charged Higgs bosons in $tH^\pm \to ttb$ at both the LHC and at a 100 TeV future collider, using a type-II two Higgs doublet model with mass degenerate heavy Higgs bosons. In the limit where $H^\pm$ couples mostly to tb, we find that the LHC has access only to relatively large effective Yukawa couplings y_{tb} when

$m_{H^\pm} > 1$ TeV — confirming and extending the expectations from Ref. [16]. Additionally, we find that supersymmetric corrections to the bottom Yukawa coupling are large, and further reduce sensitivity to a MSSM charged Higgs boson at the LHC. These findings indicate that a next-generation collider will probably be necessary to examine TeV-scale charged Higgs bosons that couple strongly to the third generation of quarks. In comparison to more optimistic predictions [24], we stress the importance of using realistic b-tagging efficiencies [28, 29] in phenomenological predictions covering TeV-scale physics.

Our particular choice of 2HDM (type-II with degenerate masses) ensures that $H^\pm tb$ is the only pertinent coupling. A less restrictive model (e.g. where $H^\pm$ couples to charm [49]), or one with alternate decay channels, such as $H^\pm \to W^\pm H$, may still be visible at the LHC given sufficient integrated luminosity. In those cases, one can convert our limit on y_{tb} to a limit on cross-section times branching fraction for the channel $tH^\pm \to ttb$ in those models.

Finally, we find a 100 TeV proton collider has the potential to close the moderate $\tan\beta$ "wedge" region below 2 TeV. While the charged Higgs-top associated channel will be background limited at such a machine, charged Higgs bosons with masses up to 6 TeV can be probed with very little dependence on model parameters (such as the sign of the μ-parameter in SUSY). Hence, a future circular collider shows great promise in shedding light on the structure of multiplets in the Higgs boson sector.

ACKNOWLEDGMENTS

We thank Carlos Wagner for his help with the SUSY Δm_b correction. This work was supported by the U.S. Department of Energy under award No. de-sc0008347.

---

[1] G. Aad *et al.* (ATLAS and CMS Collaborations), "Combined Measurement of the Higgs Boson Mass in pp Collisions at $\sqrt{s} = 7$ and 8 TeV with the ATLAS and CMS Experiments," Phys. Rev. Lett. **114**, 191803 (2015).

[2] T. D. Lee, "A Theory of Spontaneous T Violation," Phys. Rev. D **8**, 1226 (1973).

[3] P. Fayet, "Supergauge Invariant Extension of the Higgs Mechanism and a Model for the electron and Its Neutrino," Nucl. Phys. B **90**, 104 (1975).

[4] P. Fayet, "Supersymmetry and Weak, Electromagnetic and Strong Interactions," Phys. Lett. **64B**, 159 (1976).

[5] P. Fayet, "Spontaneously Broken Supersymmetric Theories of Weak, Electromagnetic and Strong Interactions," Phys. Lett. **69B**, 489 (1977).

[6] S. Dimopoulos and H. Georgi, "Softly Broken Supersymmetry and SU(5)," Nucl. Phys. B **193**, 150 (1981).

[7] H. E. Haber and G. L. Kane, "The Search for Supersymmetry: Probing Physics Beyond the Standard Model," Phys. Rept. **117**, 75 (1985).

[8] R. D. Peccei and H. R. Quinn, "CP Conservation in the Presence of Instantons," Phys. Rev. Lett. **38**, 1440 (1977).

[9] J. E. Kim, "Light Pseudoscalars, Particle Physics and Cosmology," Phys. Rept. **150**, 1 (1987).

[10] N. Turok and J. Zadrozny, "Electroweak baryogenesis in the two doublet model," Nucl. Phys. B **358**, 471 (1991).

[11] M. Joyce, T. Prokopec, and N. Turok, "Nonlocal electroweak baryogenesis. Part 2: The Classical regime," Phys. Rev. D **53**, 2958 (1996).

[12] K. Funakubo, A. Kakuto, and K. Takenaga, "The Effective potential of electroweak theory with two massless Higgs doublets at finite temperature," Prog. Theor. Phys. **91**, 341 (1994).

[13] G. C. Branco, P. M. Ferreira, L. Lavoura, M. N. Rebelo, M. Sher, and J. P. Silva, "Theory and phenomenology of two-Higgs-doublet models," Phys. Rept. **516**, 1 (2012).

[14] G. Aad *et al.* (ATLAS and CMS Collaborations), "Measurements of the Higgs boson production and decay rates and constraints on its couplings from a combined ATLAS and CMS analysis of the LHC pp collision data at $\sqrt{s} = 7$ and 8 TeV," JHEP **1608**, 045 (2016).

[15] P. M. Ferreira, J. F. Gunion, H. E. Haber, and R. Santos, "Probing wrong-sign Yukawa couplings at the LHC and a future linear collider," Phys. Rev. D **89**, no. 11, 115003 (2014).

[16] N. Craig, F. D'Eramo, P. Draper, S. Thomas, and H. Zhang, "The Hunt for the Rest of the Higgs Bosons," JHEP **1506**, 137 (2015).

[17] J. F. Gunion and H. E. Haber, "The CP conserving two Higgs doublet model: The Approach to the decoupling limit," Phys. Rev. D **67**, 075019 (2003).

[18] I. F. Ginzburg and M. Krawczyk, "Symmetries of two Higgs doublet model and CP violation," Phys. Rev. D **72** 115013 (2005).

[19] P. S. Bhupal Dev and A. Pilaftsis, "Maximally symmetric two Higgs doublet model with

natural standard model alignment," JHEP **1412**, 024 (2014), Erratum: JHEP **1511**, 147 (2015).

[20] D. Dicus, A. Stange, and S. Willenbrock, "Higgs decay to top quarks at hadron colliders," Phys. Lett. B **333**, 126 (1994).

[21] E. Asakawa, J. i. Kamoshita, A. Sugamoto, and I. Watanabe, "Production of scalar Higgs and pseudoscalar Higgs in multi-Higgs doublet models at gamma gamma colliders," Eur. Phys. J. C **14**, 335 (2000).

[22] G. Aad *et al.* (ATLAS Collaboration), "Search for charged Higgs bosons in the $H^{\pm} \to tb$ decay channel in pp collisions at $\sqrt{s} = 8$ TeV using the ATLAS detector," JHEP **1603**, 127 (2016).

[23] V. Khachatryan *et al.* (CMS Collaboration), "Search for a charged Higgs boson in pp collisions at $\sqrt{s} = 8$ TeV," JHEP **1511**, 018 (2015).

[24] J. Hajer, Y. Y. Li, T. Liu, and J. F. H. Shiu, "Heavy Higgs Bosons at 14 TeV and 100 TeV," JHEP **1511**, 124 (2015).

[25] CEPC-SPPC Study Group, "CEPC-SPPC Preliminary Conceptual Design Report. 1. Physics and Detector," IHEP-CEPC-DR-2015-01, IHEP-TH-2015-01, HEP-EP-2015-01.

[26] S. Chatrchyan *et al.* (CMS Collaboration), "Identification of b-quark jets with the CMS experiment," JINST **8**, P04013 (2013).

[27] G. Aad *et al.* (ATLAS Collaboration), "Performance of b-Jet Identification in the ATLAS Experiment," JINST **11**, P04008 (2016).

[28] K. Pedersen and Z. Sullivan, "μ_x boosted-bottom-jet tagging and Z' boson searches," Phys. Rev. D **93**, 014014 (2016).

[29] K. Pedersen, "Modified Delphes 3," [`https://github.com/keith-pedersen/delphes/tree/HighPtBTagger_Devel`].

[30] J. de Favereau *et al.* (DELPHES 3 Collaboration), "DELPHES 3, A modular framework for fast simulation of a generic collider experiment," JHEP **1402**, 057 (2014).

[31] CMS Collaboration, "A Cambridge-Aachen (C-A) based Jet Algorithm for boosted top-jet tagging," CMS-PAS-JME-09-001.

[32] M. Cacciari, G. P. Salam, and G. Soyez, "The Anti-k(t) jet clustering algorithm," JHEP **0804**, 063 (2008).

[33] Y. L. Dokshitzer, G. D. Leder, S. Moretti, and B. R. Webber, "Better jet clustering algorithms," JHEP **9708**, 001 (1997).

[34] G. Aad *et al.* (ATLAS Collaboration), "Search for $t\bar{t}$ resonances in the lepton plus jets final state with ATLAS using 4.7 fb^{-1} of pp collisions at $\sqrt{s} = 7$ TeV," Phys. Rev. D **88**, 012004 (2013).

[35] N. D. Christensen and C. Duhr, "FeynRules — Feynman rules made easy," Comput. Phys. Commun. **180**, 1614 (2009).

[36] A. Alloul, N. D. Christensen, C. Degrande, C. Duhr, and B. Fuks, "FeynRules 2.0 — A complete toolbox for tree-level phenomenology," Comput. Phys. Commun. **185**, 2250 (2014).

[37] C. Degrande, "Automatic evaluation of UV and R2 terms for beyond the Standard Model Lagrangians: a proof-of-principle," Comput. Phys. Commun. **197**, 239 (2015).

[38] C. Duhr, M. Herquet and C. Degrande "2HDM.fr" [https://feynrules.irmp.ucl.ac.be/wiki/2HDM]

[39] J. Alwall *et al.*, "The automated computation of tree-level and next-to-leading order differential cross sections, and their matching to parton shower simulations," JHEP **1407**, 079 (2014).

[40] S. Dulat *et al.*, "New parton distribution functions from a global analysis of quantum chromodynamics," Phys. Rev. D **93**, 033006 (2016).

[41] T. Sjostrand, S. Mrenna, and P. Z. Skands, "A Brief Introduction to PYTHIA 8.1," Comput. Phys. Commun. **178**, 852 (2008).

[42] T. Sjostrand, S. Mrenna, and P. Z. Skands, "PYTHIA 6.4 Physics and Manual," JHEP **0605**, 026 (2006).

[43] M. Cacciari, G. P. Salam, and G. Soyez, "FastJet User Manual," Eur. Phys. J. C **72**, 1896 (2012).

[44] G. Aad *et al.* (ATLAS Collaboration), ATL-PHYS-PUB-2015-022.

[45] CMS Collaboration, "Boosted Top Jet Tagging at CMS," CMS-PAS-JME-13-007.

[46] G. Aad *et al.* (ATLAS Collaboration), "Identification of high transverse momentum top quarks in pp collisions at $\sqrt{s} = 8$ TeV with the ATLAS detector," JHEP **1606**, 093 (2016).

[47] M. Carena, D. Garcia, U. Nierste, and C. E. M. Wagner, "Effective Lagrangian for the $\bar{t}bH^+$ interaction in the MSSM and charged Higgs phenomenology," Nucl. Phys. B **577**, 88 (2000).

[48] S. Dawson, C. Kao, and Y. Wang, "SUSY QCD Corrections to Higgs Pair Production from Bottom Quark Fusion," Phys. Rev. D **77**, 113005 (2008).

[49] W. Altmannshofer, J. Eby, S. Gori, M. Lotito, M. Martone, and D. Tuckler, "Collider signatures of flavorful Higgs bosons," Phys. Rev. D **94**, 115032 (2016).